ORIGINAL PAPER

Morphology and chemical characteristics of taste buds associated with P2X3-immunoreactive afferent nerve endings in the rat incisive papilla

Motoi Ito[1], Takuya Yokoyama[2 *], Masato Hirakawa[2], Yoshio Yamamoto[3], Wakana Sakanoue[1], Kenichi Sato[1], Tomoyuki Saino[2]

[1] Division of Dental Anesthesiology, Department of Reconstructive Oral and Maxillofacial Surgery, School of Dentistry, Iwate Medical University, Yahaba, Japan

[2] Department of Anatomy (Cell Biology), Iwate Medical University, Yahaba, Japan

[3] Laboratory of Veterinary Anatomy and Cell Biology, Faculty of Agriculture, Iwate University, Morioka, Japan

* Corresponding Author: Takuya Yokoyama, D.V.M., Ph.D.

Department of Anatomy (Cell Biology), Iwate Medical University, 1-1-1 Idaidori, Yahaba-cho, Shiwa-gun, Iwate, 028-3694, Japan

Tel.: +81-19-651-5111 (ext. 5871); Fax: +81-19-908-8006

E-mail: ytakuya@iwate-med.ac.jp

Abstract

The present study investigated the cellular components and afferent innervations of taste buds in the rat incisive papilla by immunohistochemistry using confocal scanning laser microscopy. Taste buds containing GNAT3-immmunoreactive cells were densely distributed in the lateral wall of incisive papilla forming the opening of nasoincisor ducts. GNAT3-immunoreactive cells in the taste buds were slender in shape and the tips of apical processes gathered at one point at the surface of the epithelium. The number of taste buds was 56.8 ± 4.5 in the incisive papilla. The incisive taste buds also contained ENTPD2-immunoreactive cells and synaptotagmin-1-immunoreactive cells in addition to GNAT3-immunoreactive cells. Furthermore, GNAT3-immunoreactive cells were immunoreactive to taste transduction molecules such as PLCβ2 and IP3R3. P2X3-immunoreactive subepithelial nerve fibers intruded into the taste buds, and terminated with hederiform or calix-like nerve endings attached to GNAT3-immunoreactive cells and SNAP25-immunoreactive cells. Some P2X3-immunoreactive endings were also weakly immunoreactive for P2X2. Furthermore, a retrograde tracing method using fast blue dye indicated that most of P2X3-immunoreactive nerve endings originated from the geniculate ganglia of the facial nerve. These results suggest that incisive taste buds are same as those of lingual taste buds in terms of the morphology and cellular components, and are innervated by P2X3-immunoreactive nerve endings derived from the geniculate ganglia. The incisive papilla may be the palatal taste papilla that transmits chemosensory information in the oral cavity to the geniculate ganglia via P2X3-immunoreactive afferent nerve endings.

KEY WORDS: geniculate ganglia, GNAT3, incisive papilla, P2X purinoceptor, taste buds

1. INTRODUCTION

The taste buds are the cell clusters of slender taste cells that detect chemical substances and are distributed in the lingual, palatal, and pharyngeal epithelia. In lingual taste buds, taste cells have been classified into three subtypes: type I cells (sustentacular cells), type II cells (receptor cells), and type III cells (presynaptic cells). Type I cells have lamellar cytoplasmic extensions that ensheath other taste cells. Immunohistochemically, type II cells express G protein-coupled receptors detecting for sweet, bitter or umami tastes (Zhang et al., 2003; DeFazio et al., 2006). They also contain taste transduction molecules, such as guanine nucleotide-binding protein G(t), subunit α3 (GNAT3 or α-gustducin), phospholipase C, β2-subunit (PLCβ2), inositol 1,4,5-trisphosphate receptor type 3 (IP3R3), and TRPM5 (Ruiz-Avila et al., 1995; Rössler et al., 1998; Clapp et al., 2001; Pérez et al., 2002). Type III cells form synaptic contacts with gustatory afferent nerve fibers and have been shown to express molecules associated with vesicular exocytosis, such as synaptosomal-associated protein, 25 kDa (SNAP25) and synaptotagmin-1 (Syt1, Yang et al., 2000; Kohno et al., 2005).

The palatal taste buds are distributed in three regions: soft palate, geschmachsstreifen (palatal taste stripe), and incisive papilla associated with nasoincisor ducts connecting the nasal and oral cavities in the rear of the upper incisors (Miller & Spangler, 1982). Although the exact function of incisive taste buds remains unknown, electrophysiological studies suggest that the incisive papilla near the opening of nasoincisor ducts plays a role in the sweet taste transduction (Travers et al., 1986; Travers & Norgren, 1991). Previous immunohistochemical studies have revealed that

the taste buds of the rat incisive papilla contain GNAT3-immunoreactive cells and SNAP25-immunoreactive cells (Pumplin & Getschman, 2000; El-Sharaby et al., 2001). However, the morphological characteristics and cellular component of taste buds in the incisive papilla have not yet elucidated in detail.

In lingual taste buds, adenosine 5'-triphosphate (ATP) functions as the major excitatory transmitter in the taste transduction. Nerve endings immunoreactive for P2X2/P2X3 purinoceptors were distributed in the rat lingual taste buds (Kataoka et al., 2006; Yang et al., 2012). Type II cells in the lingual taste buds released ATP in response to tastant stimulation, and the released ATP then activated afferent fibers via P2X2/P2X3 purinoceptors (see reviews, Kinnamon & Finger, 2013; Roper, 2013). On the other hand, type I cells in the lingual taste buds express ectonucleoside triphosphate diphosphohydrolase 2 (ENTPD2 or ecto-ATPase) and therefore may be involved in degrading ATP (Bartel et al., 2006; Vandenbeuch et al., 2013). However, it currently remains unknown whether P2X purinoceptors-expressing afferent nerve endings innervate taste buds in the rat incisive papilla. The regeneration experiments of taste buds in the rat incisive papilla following greater superficial petrosal nerve (GSP) transection indicated that they were innervated by GSP that projected from the geniculate ganglia (GG, St. John et al., 2003). Moreover, immunoreactivies for P2X2 and P2X3 purinoceptors have been detected in sensory neurons of the rat and mouse GG (Ishida et al., 2009). These findings suggest that taste buds in the incisive papilla are innervated by P2X purinoceptors-containing afferent nerve endings derived from GG.

In the present study, we examined the cellular components and afferent innervations of taste buds in the rat incisive papilla using immunohistochemistry with

confocal laser scanning microscopy. Various immunohistochemical markers were used for multi-labeling immunofluorescence in order to identify taste cells and elucidate the morphological relationships between these cells and P2X3-immunoreactive afferent nerve endings in the incisive taste buds. Furthermore, we also performed retrograde neurotracing using fast blue (FB) dye to identify the origin of P2X3-immunoreactive nerve endings innervating taste buds of the incisive papilla.

2. MATERIALS AND METHODS

2.1. Animal procedure

All animal experiments in the present study were approved by and conducted under the authority of the Iwate Medical University Institutional Animal Care and Use Committee (accession number #30-026). Male Wistar rats (8-10 weeks old; totally n = 40) were purchased from Japan SLC, Inc. (Slc: Wistar, Japan SLC, Hamamatsu, Japan).

2.2. Immunohistochemistry

Details of the antibodies used in the present study and their combinations are shown in Table 1-3.

Regarding cryostat sections, rats (n = 18) were transcardially perfused with Ringer's solution (200 ml) under deep anesthesia by an intraperitoneal pentobarbital injection (150 mg/kg). The incisive papillae were dissected out, and then fixed in 4% paraformaldehyde in 0.1 M phosphate buffer (pH 7.4) at 4 °C for 12-18 h. After washing with phosphate-buffered saline (PBS; pH 7.4), tissues were soaked in PBS containing 30% sucrose, frozen at -80 °C with compound medium (Tissue-Tek O.C.T. compound, Sakura Finetech, Tokyo, Japan), and then sectioned in transverse planes at a thickness of 10 μm. These sections were mounted on glass with chrome-alum gelatin and dried. Sections were incubated with non-immune donkey serum (1:50 dilution, S30, Millipore, Billerica, MA, USA) diluted with PBS containing 0.5% Triton X-100 (PBS-

T, pH 7.4) at room temperature for 30 min. After incubation with normal donkey serum, sections were then incubated with primary antibodies at 4 °C for 12 h. To penetrate antibodies, PBS-T was used as a diluent. An antibody for GNAT3 has been used as the marker of type II cells (Boughter et al., 1997), that for ENTPD2 has been used as the marker of type I cells (Bartel et al., 2006), while those for Syt1 and SNAP25 have been used as markers of type III cells in lingual taste buds (Yang et al., 2000; Kohno et al., 2005). Sections were subsequently incubated with secondary antibodies at room temperature for 2 h after rinsing with PBS. Sections were then incubated with 4',6-diamidino-2-phenylindole (DAPI) solution (1 µg/ml; Dojindo, Kumamoto, Japan) for nuclear staining. Finally, sections were coverslipped with aqueous mounting medium (Fluoromount; Diagnostic Biosystems, Pleasanton, CA, USA).

Regarding whole-mount preparations, rats (n = 12) were anesthetized by pentobarbital and transcardially perfused with Ringer's solution (200 ml) followed by the same fixative (200 ml). The incisive papillae were dissected out and further fixed at 4 °C for 12-18 h. After washing with PBS, the incisive papillae were cut longitudinally in the middle, and the submucosal tissues were removed using fine scissors under a binocular dissecting microscope to obtain whole-mount preparations of the incisive papillary mucosa. After incubation with normal donkey serum (1:50 dilution) diluted with PBS-T at room temperature for 2 h, whole-mount preparations were incubated with primary antibodies at 4 °C for at least 5 days. They were then incubated with secondary antibodies at 4 °C for 24 h, followed by an incubation with DAPI solution for nuclear staining. Preparations were mounted on glass slides coated with chrome alum-gelatin and coverslipped with aqueous mounting medium.

145 2.3. Observations

Preparations were examined with a confocal scanning laser microscope (A1R HD25; Nikon, Tokyo, Japan). Projection images were made from z-stacks of confocal images (4-55 series at 0.5-5 μm intervals) using computer software (NIS-elements; Nikon).
150 Other images were reconstructed in three-dimensional views by the alpha-blending method from intact confocal images of z-stack series. All digital images were analyzed with the use of Photoshop CC (Adobe Systems, San José, CA, USA) in addition to NIS-Elements. NIS-Elements software was also used for the analyses of the distribution and numbers of taste buds and taste cells in the incisive papilla. Values are shown as mean ±
155 SE.

2.4. Reverse transcriptase-polymerase chain reaction (RT-PCR)

RT-PCR analysis was performed to confirm the mRNA expression of the markers for
160 taste cells in the incisive papilla. Rats (n = 6) were euthanized by inhalation of carbon dioxide gas. The incisive papillae were immediately removed, placed in HEPES-buffered Ringer's solution (HR) containing 100 U/ml purified collagenase (Elastin Products, Owensville, MO, USA) and 5 mg/ml dispase (Roche Applied Science, Mannheim, Germany), and incubated for 40-60 min at 37 °C. HR contained 118 mM
165 NaCl, 4.7 mM KCl, 1.13 mM MgCl2, 1.25 mM CaCl2, 1 mM NaH_2PO_4, 5.5 mM glucose, 10 mM HEPES, and MEM amino acid solution (GIBCO, Tokyo, Japan), and

was adjusted to pH 7.4 with NaOH. The epithelial sheet of the incisive papilla was then peeled from subepithelial connective tissue, trimmed the area at which taste buds were distributed, and frozen in liquid nitrogen. Total RNA from the distribution area of taste buds in the incisive papilla was extracted using a magnetic bead method (MagExtractor; TOYOBO, Osaka, Japan). RT-PCR was performed using a QIAGEN One Step RT-PCR Kit (Qiagen, Tokyo, Japan) with gene-specific primers for ENTPD2, GNAT3, PLCβ2, IP3R3, TRPM5, Syt1, SNAP25, and β-actin as internal controls. Details of the primers used in this study are shown in Table 4. All primer pairs were designed to anchor in exons that span introns to exclude genomic DNA contamination. Reverse transcription was performed for 30 min at 50 °C, and the initial PCR activation was incubated for 15 min at 95 °C. Following reverse transcription, PCR amplification was performed 35 times as follows: 30 s at 94 °C for denaturation, 30 s at 60 °C for annealing, and 1 min at 72 °C for extension. After PCR amplification, a final extension was performed for 10 min at 72 °C. PCR end products were visualized on 2% agarose gels using ethidium bromide. The mRNA templates were omitted for negative controls.

2.5. Retrograde labeling

Rats (n = 4) were anesthetized by intraperitoneal injection of medetomidine hydrochloride (0.15 mg/kg), midazolam (2 mg/kg), and butorphanol tartrate (2.5 mg/kg), and were placed supine position to expose the incisive papilla. A retrograde tracer (0.4 µl of 2.5% FB in 10% dimethyl sulfoxide (FB; Polysciences, Warrington, PA, USA) was injected bilaterally into subepithelial tissue through mucosal epithelia of

the incisive papilla near the orifice of nasoincisor ducts at three points using a glass micropipette (inner diameter of approximately 50 μm at the tip) connected to a Hamilton micro-syringe (Hamilton Syringe Company, Anaheim, CA, USA). The injection site of FB was selected the area at which P2X3-immunoreactive nerve endings in the taste buds were observed. After surviving for 7 days, animals were fixed by transcardial perfusion with 4% paraformaldehyde as described above, and the GG were bilaterally dissected. The incisive papillae were also collected to confirm dye injection sites. Serial cryostat sections at a thickness of 20 μm were stained by immunofluorescence for P2X3. Epifluorescence microscopy (BX50; Olympus, Tokyo, Japan) was used to count FB-labeled neurons in all sections. Some sections containing FB-labeled neurons were photographed using a confocal scanning laser microscope.

3. RESULTS

3.1. Morphology and chemical characteristics of taste buds in the incisive papilla

A lower magnification view of the transverse section of the rat incisive papilla immunolabeled with GNAT3 is shown in Figure 1a. The incisive papilla was a large dome-shaped structure (1.2-1.4 mm in diameter), and formed the medial wall of the orifices of nasoincisor ducts. The nasoincisor ducts connected the nasal and oral cavities, and the orifices were observed as narrow clefts bilateral to the incisive papilla. GNAT3-immunoreactive taste buds were observed in both sides of lateral wall of the incisive papilla, but not in the subsequent ductal epithelium of nasoincisor ducts. The range of area at which the taste buds distributed was within approximately 500 μm from the palatal surface. The taste buds consisted of slender GNAT3-immunoreactive cell clusters in the stratified squamous epithelium covering incisive papilla (Figure 1b). At a higher magnification, slender GNAT3-immunoreactive cells gathered within a taste bud in the epithelial layer (Figure 1c). GNAT3-immunoreactive cells consisted of a perinuclear region with an oval nucleus and slender apical processes. The apical processes of these cells gathered at one spot and faced the oral cavity. Whole-mount preparations revealed the elliptical distribution of taste buds containing GNAT3-immunoreactive cells in the lateral wall of the incisive papilla (Figure 1d). The range of area at which the taste buds distributed was 400-600 μm in the major axis and 200-300 μm in the minor axis, and the distribution area was 0.16 ± 0.01 mm^2 in the incisive papillary mucosa (n = 5 whole-mount preparations). The numbers of taste buds with

GNAT3 immunoreactivity were 56.8 ± 4.5 in the incisive papilla.

Triple immunolabeling for GNAT3, ENTPD2, and Syt1 revealed that slender GNAT3-immunoreactive cells were arranged with ENTPD2-immunoreactive cells and Syt1-immunoreactive cells to form taste buds (Figure 2a-f). The ENTPD2 immunoreactivity appeared to be outlined cells, indicating the plasma membrane localization of the enzyme. Syt1-immunoreactive cells were spindle or pyriform in shape, and appeared to be localized in the margin within the taste buds. Horizontal sectional view of whole-mount preparations revealed the filamentous cytoplasmic processes of ENTPD2-immunoreactive cells in gaps between GNAT3-immunoreactive cells and Syt1-immunoreactive cells within the taste buds (Figure 2g). Three-dimensional reconstruction views revealed that ENTPD2-immunoreactive cells almost completely enveloped GNAT3-immunoreactive cells and a few Syt1-immunoreactive cells (Figure 2h, i). The tips of apical processes of individual cells gathered at one point at the surface of the epithelium. Certain nerve fibers were also immunoreactive to Syt1 around and within the taste buds (Figure 2c, e, f, i). The numbers of GNAT3-immunoreactive cells, ENTPD2-immunoreactive cells, and Syt1-immunoreactive cells in the taste buds were 12.8 ± 0.9, 30.0 ± 1.5, and 2.6 ± 0.2, respectively (34 taste buds). As a result, the taste buds in the incisive papilla contained 45.4 ± 2.3 cells. The ratios of GNAT3-immunoreactive cells, ENTPD2-immunoreactive cells, and Syt1-immunoreactive cells in the taste buds were 28.1%, 66.1%, and 5.8%, respectively.

In sections stained by double immunofluorescence for GNAT3 and PLCβ2 or IP3R3, GNAT3-immunoreactive cells were also immunoreactive for PLCβ2 and IP3R3 in the taste buds of the incisive papilla (Figure 3a-f). Triple immunolabeling confirmed

that slender GNAT3-immunoreactive cells were immunoreactive for both PLCβ2 and IP3R3 (Figure 3g-i).

3.2. Expression of mRNAs for taste cell markers in the taste buds of the incisive papilla

RT-PCR detected the mRNA amplification products for ENTPD2, GNAT3, PLCβ2, IP3R3, TRPM5, Syt1, and SNAP25 in extracts of the area at which taste buds distributed in the incisive papilla (Figure 4). PCR-amplified products for β-actin as internal controls were also detected. No PCR products were detected in samples without mRNA.

3.3. P2X2- and P2X3-immunoreactive nerve endings in taste buds of the incisive papilla

In sections stained by triple immunolabaling for P2X3, GNAT3, and SNAP25, subepithelial P2X3-immunoreactive nerve fibers intruded into taste buds, and branched and terminated in hederiform nerve endings associated with GNAT3-immunoreactive chemosensory cells and SNAP25-immunoreactive cells (Figure 5a-d). Higher magnification views showed that calyx-like axon terminals containing P2X3-immunoreactive punctate products surrounded along basal perinuclear regions and cytoplasmic processes of some SNAP25-immunoreactive cells (Figure 5e-h). P2X3-immunoreactive nerve endings were also immunoreactive for SNAP25 in the taste buds of the incisive papilla. In whole-mount preparations, P2X3-immunoreactive hederiform nerve endings were attached to perinuclear regions and elongated cytoplasmic processes

of GNAT3-immunoreactive cells and those of SNAP25-immunoreactive cells (Figure 5i-l).

In sections stained by double immunofluorescence for P2X3 and P2X2, weak P2X2 immunoreactivity was observed in P2X3-immunoreactive nerve endings within the taste buds (Figure 6a-c). Punctate P2X2 immunoreactivity was weak or not observed in spherical endings immunoreactive for P2X3.

3.4. Retrograde tracer study

After the injection of FB retrograde tracer into incisive papilla corresponding with the distribution of taste buds containing GNAT3-immunoreactive cells, FB-labeled neurons were observed in the GG (Figure 7). In sections of the incisive papilla including the FB injected site, most of the injected dye was observed within epithelial layer, and a small amount had diffused to the submucosa (Figure not shown). Most of FB-labeled neurons in the GG were also immunoreactive for P2X3 (Figure 7a-c). FB-labeled neurons with P2X3 immunoreactivity were small and medium in size (14-39 μm in diameter, Figure 7d-f). Based on experiments on four rats, a total of 17 neurons were labeled with FB in the GG. Of these FB-labeled neurons, 15/17 (88.2%) were immunoreactive for P2X3.

4. DISCUSSION

4.1. Cellular component of incisive taste buds

The present results showed that taste buds containing GNAT3-immunoreactive cells were distributed in the bilateral walls of the incisive papilla composing the orifice of the nasoincisor ducts, and the distribution was consistent with previous histological observations in rats (Boughter et al., 1997; El-Sharaby et al., 2001). GNAT3-immunoreactive cells were closely arranged in the taste buds and projected apical cytoplasmic processes reaching the lumen of the oral cavity. The morphology of these cells appeared to resemble GNAT3-immunoreactive type II cells in the rat lingual taste buds (Boughter et al., 1997; Pumplin & Getschman, 2000). Furthermore, RT-PCR detected the expression of PLCβ2, IP3R3, and TRPM5 in the incisive taste buds, and GNAT3-immunoreactive cells composing taste buds were immunoreactive for PLCβ2 and IP3R3. Since PLCβ2, IP3R3, and TRPM5 are the important taste-signaling molecules of type II cells in the lingual taste buds (Rössler et al., 1997; Clapp et al., 2001; Qian et al., 2018), GNAT3-immunoreactive cells in the incisive taste buds may be gustatory receptor cells activated by chemical stimuli in the oral cavity, similar to type II cells. In addition to GNAT3-immunoreactive cells, the incisive taste buds also contained ENTPD2-immunoreactive cells and Syt1- or SNAP25-immunoreactive cells, and apical cytoplasmic processes of these cells appeared to gather at one point. In lingual taste buds, ENTPD2 has been identified as an immunohistochemical marker for type I cells (Bartel et al., 2006), whereas Syt1 and SNAP25 have been identified as

those for type III cells (Yang et al., 2000, Kohno et al., 2005). Thus, ENTPD2-immunoreactive cells and Syt1-immunoreactive cells observed in the incisive taste buds may be identical to type I cells and type III cell in the lingual taste buds, respectively. The ratios of GNAT3-immunoreactive cells, ENTPD2-immunoreactive cells, and Syt1-immunoreactive cells in the incisive taste buds were similar to those of taste cells in the lingual taste buds (Roper & Chandhari, 2017; Yang et al., 2020). However, incisive taste buds appeared to be smaller in cell number than lingual taste buds which contain 50-100 cells (Chaudhari & Roper, 2010; Roper, 2013). We concluded that the morphology and cellular components of the incisive taste buds are fundamentally same as those of lingual taste buds, although it is unknown whether they are involved with cognition of the chemical substances or not.

4.2. P2X3-immunoreactive afferent nerve endings in incisive taste buds

The present study revealed that incisive taste buds received afferent innervation of P2X3-immunoreactive hederiform nerve endings. Physiological experiments using ATP-biosensor cells revealed that type II cells of the lingual taste buds released ATP through pannexin-1 hemichannels after taste stimuli (Huang et al., 2007). The close appositions between GNAT3-immunoreactive cells and P2X3-immunoreactive nerve endings suggest that the activation of these cells induces the release of ATP in order to transmit afferent nerve endings. Since P2X3-imunoreactive nerve endings contained a few P2X2 immunoreactivities with P2X3-immunoreactive puncta, GNAT3-immunoreactive cells may activate nerve endings via the P2X3 homomeric, and slightly

via P2X2/P2X3 heteromeric channels. In lingual taste buds, type I cells expressed the plasma membrane-bound nucleatidase, ENTPD2, that hydrolyzed extracellular ATP to adenosine diphosphate in order to remove excess transmitter from the extracellular space (Bartel et al., 2006; Vandenbeuch et al., 2013). These findings suggests that ENTPD2-immunoreactive cells regulate the chemosensory transmission from GNAT3-immunoreactive cells to P2X3-immunoreactive nerve endings by degrading extracellular ATP. Furthermore, the close relationship between SNAP25-immunoreactive cells and the calyx-like terminals of P2X3-immunoreactive nerves suggests that ATP also plays a sensory transmission between them. Previous studies reported that type III cells released serotonin, but not ATP in lingual taste buds (Huang et al., 2005, 2007), while Kinnamon & Finger, (2013) pointed out the possibility of co-release of ATP with serotonin and GABA. Further studies on ATP-mediated transmission between SNAP25-immunoreactive cells and P2X3-immunoreactive nerve endings in the incisive taste buds are needed. On the other hand, P2X3-immunoreactive nerve endings with SNAP25 immunoreactivity may have an efferent role in addition to a sensory role. In the mouse circumvallate papilla, immunoreactivity for the vesicular glutamate transporter 1 (VGLUT1) and VGLUT2, vesicle loading proteins for the exocytosis of glutamate, were localized in gustatory nerve fibers innervating taste buds, and glutamate increased intracellular calcium of type III cells, but not of type II cells (Vandenbeuch et al., 2010). Although it remains unknown whether VGLUTs are expressed in P2X3-immunoreactive nerve endings innervating incisive taste buds, the secretions of SNAP25-immunoreactive cells may be modulated by glutamate released from these nerve endings.

The results of retrograde tracing with FB suggest that P2X3-immunoreactive nerve endings innervating incisive taste buds are derived from GG. Previous studies using rats have reported that incisive taste buds are remarkably decreased or abolished after the bilateral transection of GSP that projected from the GG (St. John et al., 2003; Jiang et al., 2008). These findings suggest that chemosensory information generated by incisive taste buds is transmitted to the GG via the GSP. On the other hand, FB-labeled GG neurons without P2X3 immunoreactivity appeared to express another chemical coding, for example, transient receptor potential ankyrin 1 and vanilloid 1, AMPA receptor subunits GluR2/3, and tyrosine kinase receptors trkB and trkC, as reported by immunohistochemistry in the rat GG (Cho & Farbman, 1999; Caicedo et al., 2004; Katsura et al., 2006).

4.3. Functional considerations

The shape of the incisive papilla containing taste buds on bilateral walls was histologically resembled that of circumvallate papilla of the tongue. The incisive papilla may be the taste papilla of the hard palate, similar to the circumvallate papilla. Since the incisive papilla was situated in the most anterior field of the rat palate, the incisive taste buds may be suitable for detecting immediately chemical substances ingested in the oral cavity. On the other hand, the nasoincisor ducts connected nasal and oral cavities, and opened bilateral to the incisive papilla. Chemical substances that stimulate the incisive taste buds may be washed away by the mucus that flows from the nasal cavity through the nasoincisor ducts, similar to saliva secreted from von Ebner’s glands into the clefts

of the circumvallate taste buds. Electrophysiological studies reported that sweet taste stimulation in the rat incisive papilla near the opening of the nasoincisor ducts induced an increase of neuronal responses in the nucleus of the solitary tract (Travers et al., 1986; Travers & Norgren, 1991). Travers et al., (1986) also compared the differences in the neuronal responses to sweet, salty, sour, and bitter: sucrose evoked the greatest neuronal activity, followed by NaCl, HCl, and quinine hydrochloride. Since type II cells in the lingual taste buds were activated by sweet stimuli such as sucrose (DeFazio et al., 2006), incisive taste buds containing GNAT3-immunoreactive cells may be activated primarily by sweet stimuli, and transmit chemosensory signals to the central nervous system via P2X3-immunoreactive afferent nerve endings derived from GG. Further studies on the electrophysiological and pharmacological properties of cellular components and P2X3-immunoreactive nerve endings are needed in order to clarify the precise functions of taste buds in the rat incisive papilla.

ACKNOWLEDGEMENTS

The authors are grateful to Ms. Sawa Takita, the medical student at Iwate Medical University for her technical support with the immunohistochemistry. This work was supported by Grants-in-Aid from the Japan Society for the Promotion of Science to Takuya Yokoyama (JP19K16482).

CONFLICT OF INTEREST

The authors declare that they have no conflict of interest.

AUTHOR CONTRIBUTIONS

All authors had full access to all the data in the study and take responsibility for its integrity and the accuracy of the data analysis. **Takuya Yokoyama:** Study concept and design. **Motoi Ito, Takuya Yokoyama, Masato Hirakawa, Yoshio Yamamoto, and Wakana Sakanoue:** Acquisition of data. **Motoi Ito, Takuya Yokoyama, Masato Hirakawa, Yoshio Yamamoto, Kenichi Sato, and Tomoyuki Saino:** Analysis and interpretation of data. **Motoi Ito:** Drafting of the manuscript. **Takuya Yokoyama:** Critical revision of the manuscript and approval of the article.

DATA AVAILABILITY STATEMENT

The data that support the findings of this study are available from the corresponding author upon reasonable request.

ORCID

Takuya Yokoyama, https://orcid.org/0000-0003-3384-0623

Yoshio Yamamoto, https://orcid.org/0000-0002-6352-6013

Tomoyuki Saino, https://orcid.org/0000-0001-6360-9516

REFERENCES

Bartel, D.L., Sullivan, S.L., Lavoie, E.G., Sevigny, J. & Finger, T.E. (2006) Nucleoside triphosphate diphosphohydrolase-2 is the ecto-ATPase of type I cells in taste buds. *The Journal of Comparative Neurology*, 497, 1-12.

Boughter, J.D. Jr., Pumplin, D.W., Yu, C., Christy, R.C. & Smith, D.V. (1997) Differential expression of alpha-gustducin in taste bud populations of the rat and hamster. *The Journal of Neuroscience*, 17, 2852-2858.

Caicedo, A., Zucchi, B., Pereira, E. & Roper, S.D. (2004) Rat gustatory neurons in the geniculate ganglion express glutamate receptor subunits. *Chemical Senses*, 29. 463-471.

Chaudhari, N. & Roper, S.D. 2010. The cell biology of taste. *The Journal of Cell Biology*, 190, 285-296.

Cho, T.T. & Farbman, A.I. 1999. Neurotrophin receptors in the geniculate ganglion. *Brain Research. Molecular Brain Research*, 68, 1-13.

Clapp, T.R., Stone, L.M., Margolskee, R.F. & Kinnamon, S.C. (2001) Immunocytochemical evidence for co-expression of Type III IP_3 receptor with signaling components of bitter taste transduction. *BMC Neuroscience*, 2, 6.

DeFazio, R.A., Dvoryanchikov, G., Maruyama, Y., Kim, J.W., Pereira, E., Roper, S.D. & Chaudhari, N. (2006) Separate populations of receptor cells and presynaptic cells in mouse taste buds. *The Journal of Neuroscience*, 26, 3971-3980.

El-Sharaby, A., Ueda, K., Kurisu, K. & Wakisaka, S. (2001) Development and maturation of taste buds of the palatal epithelium of the rat: histological and immunohistochemical study. *Anatomical Record*, 263, 260-268.

Honer, W.G., Hu, L. & Davies, P. (1993) Human synaptic proteins with a heterogeneous distribution in cerebellum and visual cortex. *Brain Research*, 609, 9-20.

Huang, L.-C., Greenwood, D., Thorne, P.R. & Housley, G.D. (2005) Developmental regulation of neuron specific $P2X_3$ receptor expression in the rat cochlea. *The Journal of Comparative Neurology*, 484, 133-143.

Huang, Y.J., Maruyama, Y., Dvoryanchikov, G., Pereira, E., Chaudhari, N. & Roper, S.D. (2007) The role of pannexin 1 hemichannels in ATP release and cell-cell communication in mouse taste buds. *Proceedings of the National Academy of Sciences of the United States of America*, 104, 6436-6441.

Ishida, Y., Ugawa, S., Ueda, T., Yamada, T., Shibata, Y., Hondoh, A., Inoue, K., Yu, Y. & Shimada, S. (2009) $P2X_2$- and $P2X_3$-positive fibers in fungiform papillae originate from the chorda tympani but not the trigeminal nerve in rats and mice. *The Journal of Comparative Neurology*, 514, 131-144.

Jiang, E., Blonde, G., Garcea, M. & Spector, A.C. (2008) Greater superficial petrosal nerve transection in rats does not change unconditioned licking responses to putatively sweet taste stimuli. *Chemical Senses*, 33, 709-723.

Kataoka, S., Toyono, T., Seta, Y. & Toyoshima, K. (2006) Expression of ATP-gated P2X3 receptors in rat gustatory papillae and taste buds. *Archives of Histology and Cytology*, 69, 281-288.

Katsura, H., Tsuzuki, K., Noguchi, K. & Sakagami, M. (2006) Differential expression of capsaicin-, menthol-, and mustard oil-sensitive receptors in naive rat geniculate ganglion neurons. *Chemical Senses*, 31, 681-688.

Kinnamon, S.C. & Finger, T.E. (2013) A taste for ATP: neurotransmission in taste buds. *Frontiers in Cellular Neuroscience*, 7, 264.

Kohno, R., Toyono, T., Seta, Y., Kataoka, S., Yamaguchi, K. & Toyoshima, K. (2005) Expression of synaptotagmin 1 in the taste buds of rat gustatory papillae. *Archives of Histology and Cytology*, 68, 235-241.

Miller, I.J. Jr. & Spangler, K.M. (1982) Taste bud distribution and innervation on the palate of the rat. *Chemical Senses*, 7, 99-108.

Pérez, C.A., Huang, L., Rong, M., Kozak, J.A., Preuss, A.K., Zhang, H., Max, M. & Margolskee, R.F. (2002) A transient receptor potential channel expressed in taste receptor cells. *Nature Neuroscience*, 5, 1169-1176.

Pumplin, D.W. & Getschman, E. (2000) Synaptic proteins in rat taste bud cells: appearance in the Golgi apparatus and relationship to alpha-gustducin and the Lewis^{b} and A antigens. *The Journal of Comparative Neurology*, 427, 171-184.

Qian, J., Mummalaneni. S., Grider, J.R., Damaj, M.I. & Lyall, V. (2018) Nicotinic acetylcholine receptors (nAChRs) are expressed in Trpm5 positive taste receptor cells (TRCs). *PLoS One*, 13, e0190465.

Roper, S.D. (2013) Taste buds as peripheral chemosensory processors. *Seminars in Cell & Developmental Biology*, 24, 71-79.

Roper, S.D. & Chaudhari, N. (2017) Taste buds: cells, signals and synapses. *Nature Reviews. Neuroscience*, 18, 485-497.

Rössler, P., Kroner, C., Freitag, J., Noè, J. & Breer, H. (1998) Identification of a phospholipase C β subtype in rat taste cells. *European Journal of Cell Biology*, 77, 253-261.

Ruiz-Avila, L., McLaughlin, S.K., Wildman, D., McKinnon, P.J., Robichon, A., Spickofsky, N. & Margolskee, R.F. (1995) Coupling of bitter receptor to phosphodiesterase through transducin in taste receptor cells. *Nature*, 376, 80-85.

St John, S.J., Garcea, M. & Spector, A.C. (2003) The time course of taste bud regeneration after glossopharyngeal or greater superficial petrosal nerve transection in rats. *Chemical Senses*, 28, 33-43.

Travers, S.P. & Norgren, R. (1991) Coding the sweet taste in the nucleus of the solitary tract: differential roles for anterior tongue and nasoincisor duct gustatory receptors in the rat. *Journal of Neurophysiology*, 65, 1372-1380.

Travers, S.P., Pfaffmann, C. & Norgren, R. (1986) Convergence of lingual and palatal gustatory neural activity in the nucleus of the solitary tract. *Brain Research*, 365, 305-320.

Vandenbeuch, A., Anderson, C.B., Parnes, J., Enjyoji, K., Robson, S.C., Finger, T.E. & Kinnamon, S.C. (2013) Role of the ectonucleotidase NTPDase2 in taste bud function. *Proceedings of the National Academy of Sciences of the United States of America*, 110, 14789-14794.

Vandenbeuch, A., Tizzano, M., Anderson, C.B., Stone, L.M., Goldberg, D. & Kinnamon, S.C. (2010) Evidence for a role of glutamate as an efferent transmitter in taste buds. *BMC Neuroscience*, 11, 77.

Yang, R., Crowley, H.H., Rock, M.E. & Kinnamon, J.C. (2000) Taste cells with synapses in rat circumvallate papillae display SNAP-25-like immunoreactivity. *The Journal of Comparative Neurology*, 424, 205-215.

Yang, R., Dzowo, Y.K., Wilson, C.E., Russell, R.L., Kidd, G.J., Salcedo, E., Lasher, R.S, Kinnamon, J.C. & Finger, T.E. (2020) Three-dimensional reconstructions of mouse circumvallate taste buds using serial blockface scanning electron microscopy: I. Cell types and the apical region of the taste bud. *The Journal of Comparative Neurology*, 528, 756-771.

Yang, R., Montoya, A., Bond, A., Walton, J. & Kinnamon, J.C. (2012) Immunocytochemical analysis of P2X2 in rat circumvallate taste buds. *BMC Neuroscience*, 13, 51.

Zhang, Y., Hoon, M.A., Chandrashekar, J., Mueller, K.L., Cook, B., Wu, D., Zuker, C.S. & Ryba, N.J.P. (2003) Coding of sweet, bitter, and umami tastes: different receptor cells sharing similar signaling pathways. *Cell*, 112, 293-301.

Figure legends

FIGURE 1 Distribution of taste buds containing GNAT3-immunoreactive cells in the rat incisive papilla (IP). Confocal projection images are made from 8 images at 2 μm intervals in (a), 24 images at 1 μm intervals in (b), 9 images at 1 μm intervals in (c), and 5 images at 5 μm intervals in (d), respectively. (a-c) Cryostat sections of the IP stained by GNAT3. (a) The IP contains GNAT3-immunoreactive taste buds (*arrowheads*) in the bilateral wall composing the opening of nasoincisor ducts, but not in the subsequent ductal epithelium (*asterisks*). (b) Taste buds containing GNAT3-immunoreactive cells within the stratified squamous epithelium covering IP near the opening of nasoincisor duct (*arrow*). (c) A higher magnification shows spindle GNAT3-immunoreactive cells gather to form a taste bud in the epithelial layer. (d) A whole-mount preparation of the incisive papillary mucosa reveals the dense distribution of taste buds containing GNAT3-immunoreactive cells. Nuclei are labeled by DAPI (*blue*)

FIGURE 2 Triple immunolabeling for GNAT3 (Alexa488, *green*), ENTPD2 (Cy3, *red*), and Syt1 (Alexa647, *white*). Confocal projection images and three-dimensional views are made from 12 images and 55 images at 1 μm intervals in (a-f) and (h, i), respectively. (a-f) Taste buds containing GNAT3-immunoreactive cells, ENTPD2-immunoreactive cells (*asterisks* in b, d, f), and a few Syt1-immunoreactive cells (*arrowheads* in c, e, f) in the cryostat section. (g) A horizontal section of cell clusters selected from z-stack series in a whole-mount preparation. ENTPD2-immunoreactive cells fill a gap between GNAT3-immunoreactive cells and Syt1-immunoreactive cells

by lamellar cytoplasmic processes in the taste buds. (h, i) Three-dimensional reconstruction views of whole-mount preparations. ENTPD2-immunoreactive cells wrap around the taste bud composed of GNAT3-immunoreactive cells and Syt1-immunoreactive cells (*arrowheads* in i) in a dome-like fashion. The taste bud contains 20 GNAT3-immunoreactive cells, 41 ENTPD2-immunoreactive cells, and 4 Syt1-immunoreactive cells, respectively. In (a-c) and (g), nuclei are labeled by DAPI (*blue*)

FIGURE 3 Double or triple immunofluorescence for GNAT3 with PLCβ2 and/or IP3R3. Projection images are made from 8, 9, and 12 images at 1 μm intervals in (a-c), (d-f) and (g-i), respectively. (a-c) GNAT3-immunoreactive cells (Alexa488, *green*) in the cell cluster are immunoreactive for PLCβ2 (Cy3, *red*). (d-f) GNAT3-immunoreactive cells (Alexa488, *green*) in the cluster are also immunoreactive for IP3R3 (Cy3, *red*). (g-i) GNAT3-immunoreactive cells (Alexa488, *green*) in the cell cluster are immunoreactive for both IP3R3 (Cy3, *red*) and PLCβ2 (Alexa647, *white*). Nuclei are labeled by DAPI (*blue*)

FIGURE 4 RT-PCR analysis for mRNAs of the markers for taste cells in the incisive papilla. PCR-amplified products for ENTPD2 (marker for type I cells), GNAT3, PLCβ2, IP3R3, TRPM5 (markers for type II cells), Syt1, and SNAP25 (markers for type III cells) are detected in the extracts of the distribution area of incisive taste buds. PCR-amplified products are not detected in the negative controls. The expected band sizes (bp) of the PCR products are as follows: ENTPD2 (333), β-actin (276), GNAT3 (372), PLCβ2 (203), IP3R3 (458), TRPM5 (240), Syt1 (201), and SNAP25 (264)

FIGURE 5 Triple immunolabeling for P2X3 (Alexa488, *green*), GNAT3 (Cy3, *red*), and SNAP25 (Alexa647, *white*). Confocal projection images and three-dimensional views are made from 20 images at 0.5 μm intervals and 54 images at 1 μm intervals in (a-h) and (k, l), respectively. (a-d) P2X3-immunoreactive hederiform nerve endings are in close contact with GNAT3-immunoreactive cells and SNAP25-immunoreactive cells in the taste buds. (e-h) High power views of the *arrowheads* in (a-d) show P2X3- and SNAP25-immmunoreactive calyx-like axon terminals surrounding SNAP25-immunoreactive cells. (I, j) Taste buds in whole-mount preparations of the incisive papilla. Horizontal section (i) of taste buds selected from z-stack series, and the sectional view (j) at the dotted line indicated in (i). P2X3-immunoreactive nerve endings are distributed between GNAT3-immunoreactive cells and SNAP25-immunoreactive cells. (k, l) Three-dimensional reconstruction views of whole-mount preparations. P2X3-immunoreactive nerve endings are attached to GNAT3-immunoreactive cells (*arrows*) and SNAP25-immunoreactive cells (*arrowheads* in i) in the taste buds. In (d, h) and (I, j), nuclei are labeled by DAPI (*blue*)

FIGURE 6 Double immunofluorescence for P2X3 and P2X2. Confocal projection images are made from 18 images at 0.5 μm intervals. (a-c) P2X3-immunoreactive spherical nerve terminals innervating incisive taste buds are also immunoreactive for P2X2 (*arrows*), whereas some terminals are not (*arrowheads*). In (c), nuclei are labeled by DAPI (*blue*)

FIGURE 7 Fast blue (FB)-labeled neurons in the geniculate ganglia (GG) after its injection into the incisive papillary mucosa. (a-c) Most of FB-labeled neurons in the GG is immunoreactive for P2X3 (*arrows*). VII and GSP indicate facial nerve and greater superficial petrosal nerve, respectively. (d-f) Higher magnifications show that FB-labeled neuron in the GG is immunoreactive for P2X3 (*arrow*), whereas the other neuron is not (*arrowhead*)

TABLE 1 Primary antibodies used in the present study

No.	Antibody against	Immunogen	Manufacturer; host; catalog number; RRID	Dilution
1	Guanine nucleotide-binding protein G(t), subunit α3 (GNAT3)	Synthetic peptide (KNQFLDLNLKKEDKE), 304-318 amino acid sequence of human GNAT3	Abcam (Cambridge, UK); goat polyclonal; ab113664; AB_10866449	1:1,000
2	Guanine nucleotide-binding protein G(t), subunit α3 (GNAT3)	Peptide fragment containing 93-113 amino acid sequence of rat GNAT3	Santa Cruz Biotechnology (Dallas, TX, USA); sc-395; rabbit polyclonal; AB_673678	1:500
3	Ectonucleoside triphosphate diphosphohydrolase 2 (ENTPD2)	26-462 amino acid sequence of CHO-derived recombinant mouse CD39L1/ENTPD2	R&D Systems (Minneapolis, MN, USA); sheep polyclonal; AF5797; AB_10572702	1:200
4	Synaptotagmin-1 (Syt1)	Rat brain synaptic plasma membranes	R&D Systems (Minneapolis, MN, USA); mouse monoclonal; MAB4364; AB_2199304	1:1,000
5	Phospholipase C, β2-subunit (PLCβ2)	Synthetic peptide (QDPLIAKADAQ), 1170-1181 amino acid sequence of human PLCβ2	Santa Cruz Biotechnology (Dallas, TX, USA); rabbit polyclonal; sc-206; AB_632197	1:500
6	Inositol 1,4,5-trisphosphate receptor, type 3 (IP3R3)	Synthetic peptide, 22-230 amino acid sequence of human IP3R3	BD Biosciences (San Jose, CA, USA); mouse monoclonal; 610312; AB_397704	1:100
7	P2X3 purinoceptor (P2X3)	Synthetic peptide (VEKQSTDGAYSIGH), 383-397 amino acid sequence of rat P2X3	Neuromics (Edina, MN, USA); rabbit polyclonal; RA10109; AB_2157930	1:500
8	Synaptosomal-associated protein, 25 kDa (SNAP25)	Crude human synaptic immunoprecipitated, (characterize by Honer et al., 1993)	Bio-Rad (Hercules, CA, USA); mouse monoclonal; MCA1308; AB_322417	1:1,000
9	P2X2 purinoceptor (P2X2)	Synthetic peptide (DSTSTDPKGLAQL), 460-472 amino acid sequence of rat P2X2	Neuromics (Edina, MN, USA); guinea pig polyclonal; GP14106; AB_2299063	1:5,000

The antibody numbers in this table are also used in Table 3.

TABLE 2 Secondary antibodies used in the present study

Letter	Antibody against	Host	Catalog number	RRID	Dilution
a	Alexa Fluor 488-labeled anti-goat IgG	Donkey	705-545-147	AB_2336933	1:200
b	Alexa Flour 488-labeled anti-rabbit IgG	Donkey	711-545-152	AB_2313584	1:200
c	Cy3-labeled anti-sheep IgG	Donkey	713-165-147	AB_2315778	1:200
d	Cy3-labeled anti-rabbit IgG	Donkey	711-165-152	AB_2307443	1:200
e	Cy3-labeled anti-mouse IgG	Donkey	715-165-151	AB_2315777	1:200
f	Cy3-labeled anti-goat IgG	Donkey	705-165-147	AB_2307351	1:200
g	Cy3-labeled anti-guinea pig IgG	Donkey	706-165-148	AB_2340460	1:200
h	Alexa Flour 647-labeled anti-mouse IgG	Donkey	715-605-151	AB_2340863	1:200
i	Alexa Flour 647-labeled anti-rabbit IgG	Donkey	711-605-152	AB_2492288	1:200

The antibody letters in this table are also used in Table 3.

All antibodies are supplied by Jackson ImmunoResearch (West Grove, PA, USA).

TABLE 3 Combinations of antibodies for immunofluorescence

Combination	Primary antibody 1	Secondary antibody 1	Primary antibody 2	Secondary antibody 2	Primary antibody 3	Secondary antibody 3	
GNAT3	1	a	-	-	-	-	Figure 1
GNAT3/ENTPD2/Syt1	2	b	3	c	4	h	Figure 2
GNAT3/PLCβ2	1	a	5	d	-	-	Figure 3a-c
GNAT3/IP3R3	1	a	6	e	-	-	Figure 3d-f
GNAT3/IP3R3/PLCβ2	1	a	6	e	5	i	Figure 3g-i
P2X3/GNAT3/SNAP25	7	b	1	f	8	i	Figure 5
P2X3/P2X2	7	b	9	g	-	-	Figure 6
P2X3	7	b					Figure 7

Numbers and letters are shown in Tables 1 and 2.

TABLE 4 Primers for RT-PCR

mRNA (Accession #)	Primer Sequences	Position	Exon #	Product length
ENTPD2	5'-GGGCTCTTCACACACATCCA-3' (sense)	139-158	2	393 bp
(NM_172030)	5'-AGCAGGTAGTTGGCAGTCAC-3' (antisense)	512-531	4	
GNAT3	5'-AGAACTGGAGAAGAAGCTTCAGG -3' (sense)	164-186	1	372 bp
(NM_173139)	5'-TCGAAGCAGGCTTGAATTCCT -3' (antisense)	515-535	4	
PLCβ2	5'- CTGTCCTGTTGCCCCCTAAG-3' (sense)	115-134	1	203 bp
(NM_053478)	5'- GGCAAACTTCCCAAAGCGAG-3' (antisense)	298-317	3	
IP3R3	5'- CGAGGTGGAAACCTTCGTGA-3' (sense)	1974-1993	16	458 bp
(NM_013138)	5'- CCGCCATGCATAGGAAAAGC-3' (antisense)	2412-2431	19	
TRPM5	5'-CACAAGCAGCTGGGTCCTAA -3' (sense)	2557-2576	17	240 bp
(NM_001191896)	5'- AAGAGAGCAGTTCACACGGG-3' (antisense)	2777-2796	19	
Syt1	5'-AGCCATAGTTGCGGTCCTTTTA-3' (sense)	531-552	5	201 bp
(NM_001033680)	5'-CCATCAGTCAGTCCGGTTTCA-3' (antisense)	711-731	6	
SNAP25	5'-GGGCAATAATCAGGATGGAGTAGT-3' (sense)	524-547	6	264 bp
(NM_001270575)	5'-TCAATTCTGGTTTTGTTGGAGTCAG-3' (antisense)	763-787	8	
β-actin	5'-TACAACCTTCTTGCAGCTCCTC-3' (sense)	25-46	1	276 bp
(NM_031144)	5'-GCCGTGTTCAATGGGGTACT-3' (antisense)	281-300	3	

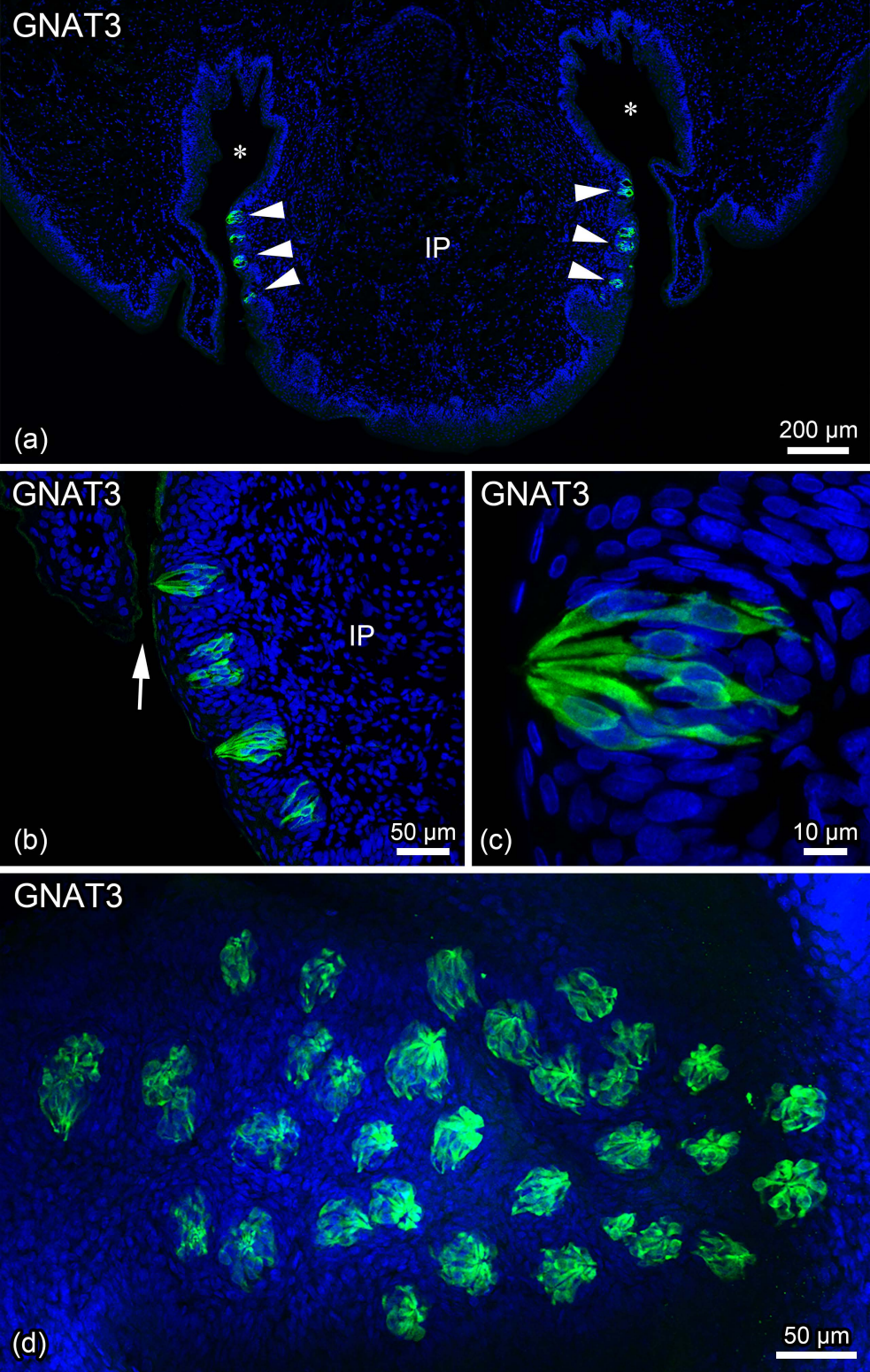
GNAT3
*
*
IP
(a)
200 μm
GNAT3
IP
(b)
50 μm
GNAT3
(c)
10 μm
GNAT3
(d)
50 μm

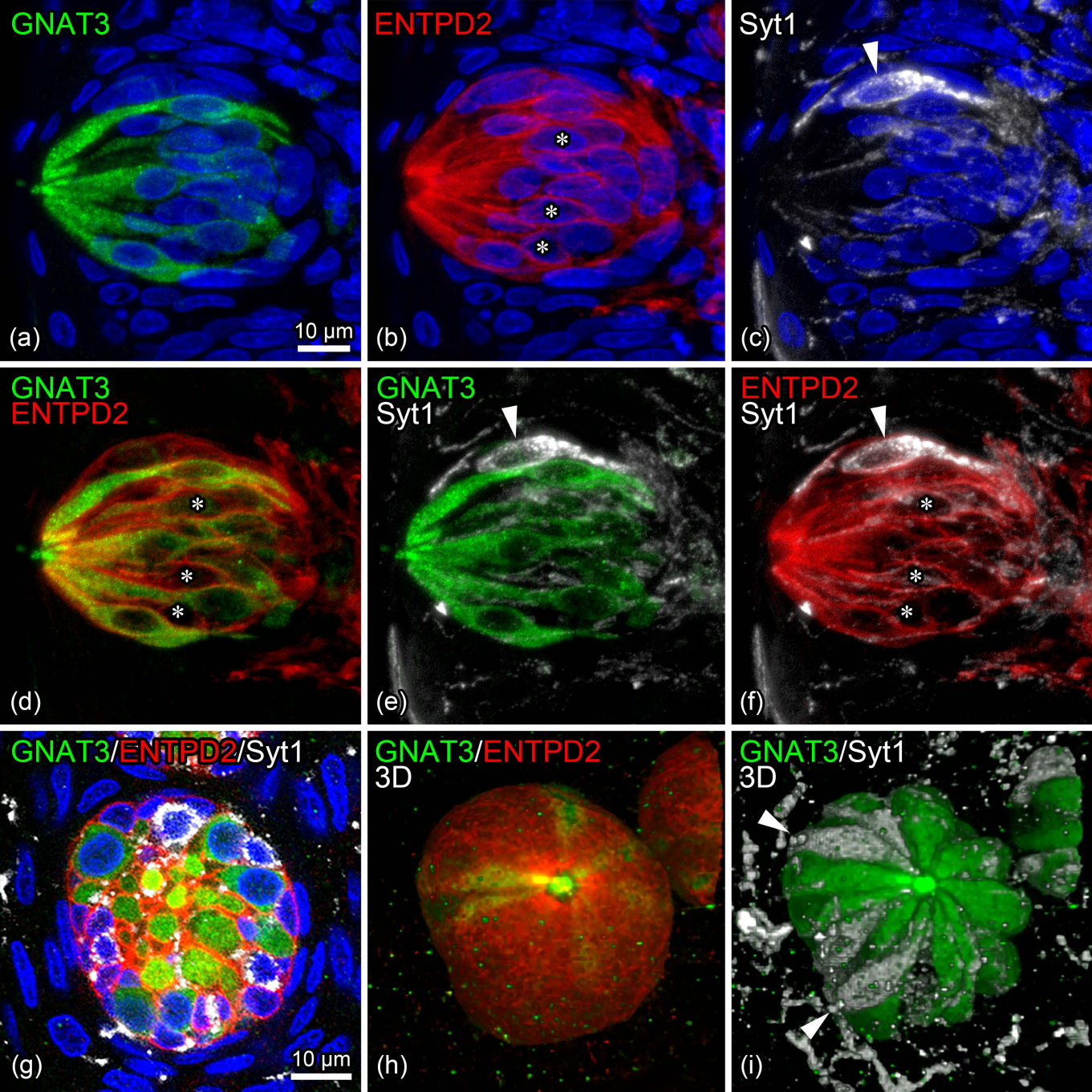
GNAT3
(a)
10 µm
ENTPD2
(b)
Syt1
(c)
GNAT3
ENTPD2
(d)
GNAT3
Syt1
(e)
ENTPD2
Syt1
(f)
GNAT3/ENTPD2/Syt1
(g)
10 µm
GNAT3/ENTPD2
3D
(h)
GNAT3/Syt1
3D
(i)

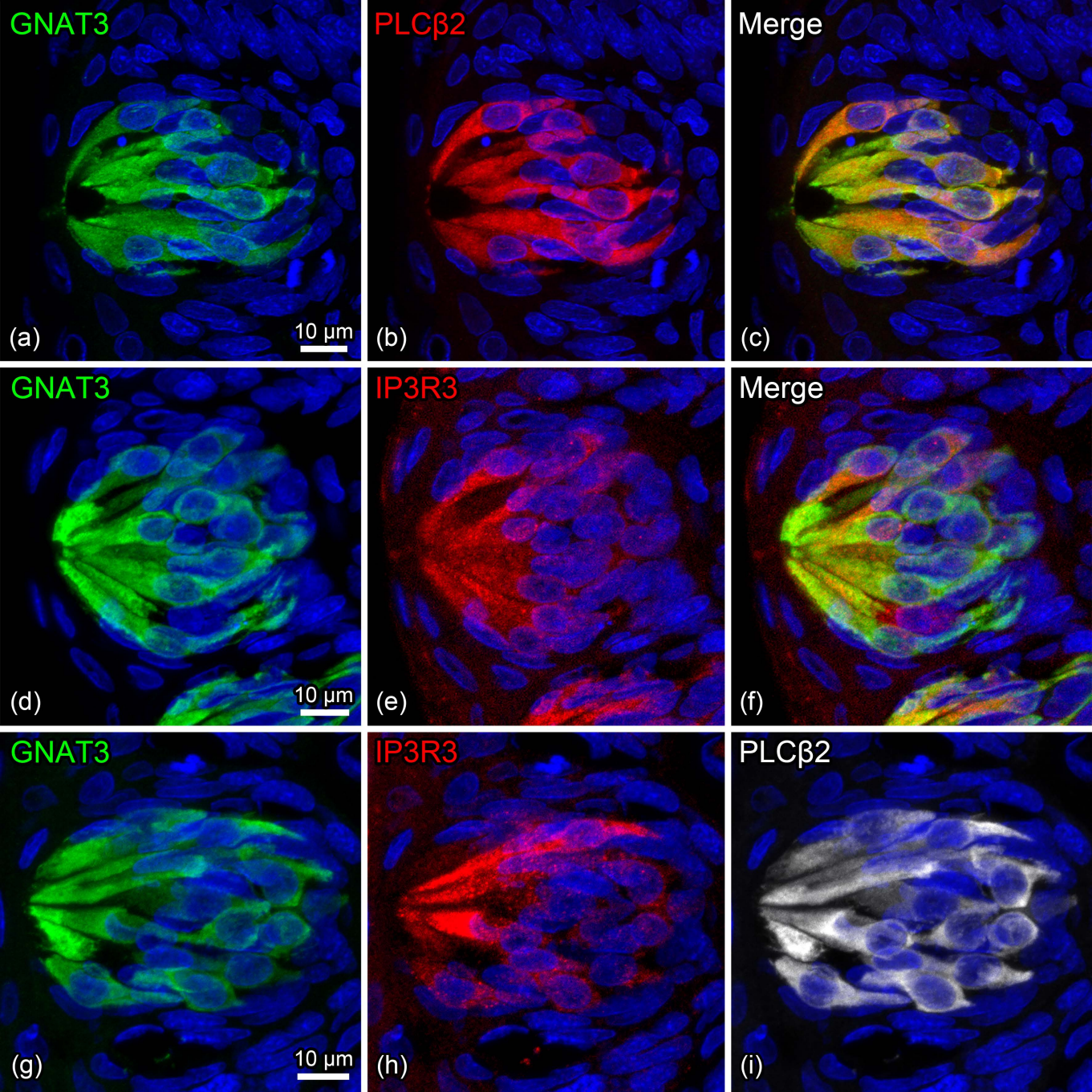
GNAT3
PLCβ2
Merge
(a)
10 μm
(b)
(c)
GNAT3
IP3R3
Merge
(d)
10 μm
(e)
(f)
GNAT3
IP3R3
PLCβ2
(g)
10 μm
(h)
(i)

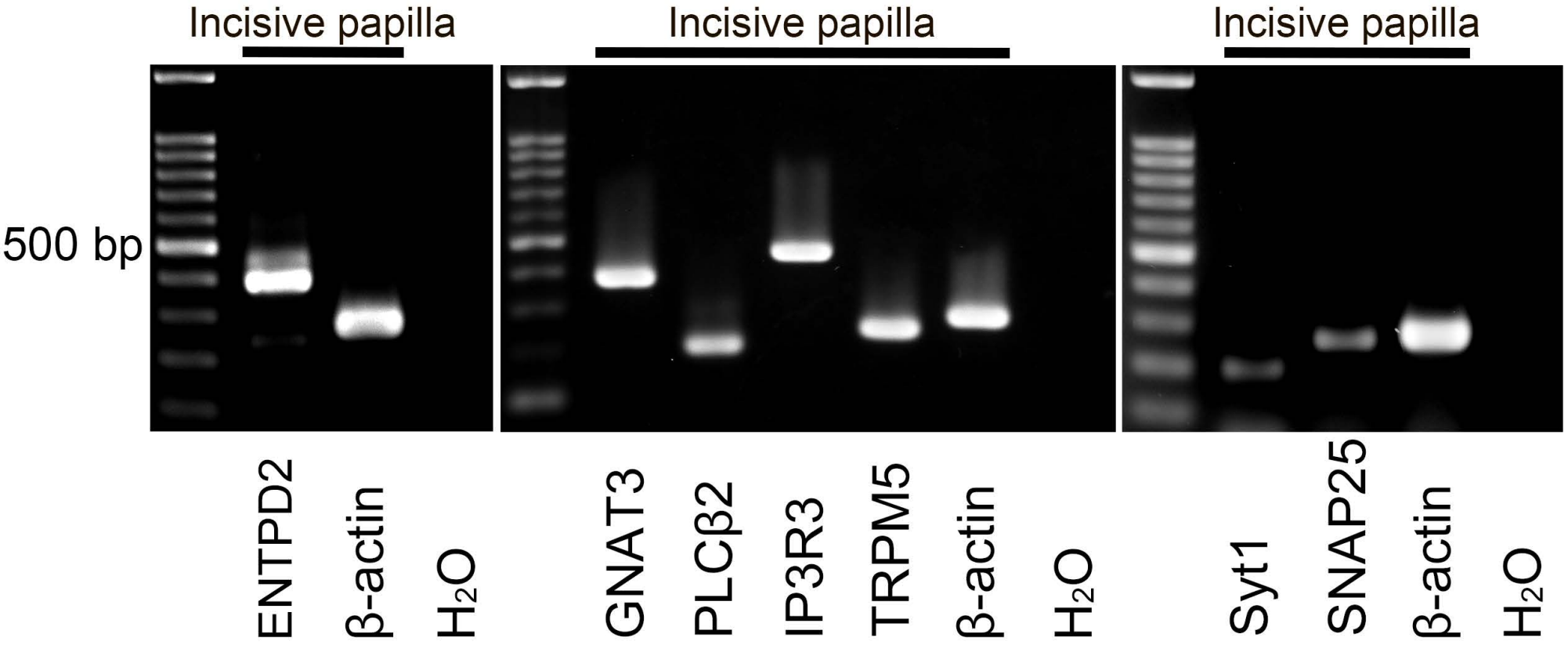
Incisive papilla
Incisive papilla
Incisive papilla
500 bp
ENTPD2
β-actin
H2O
GNAT3
PLCβ2
IP3R3
TRPM5
β-actin
H2O
Syt1
SNAP25
β-actin
H2O

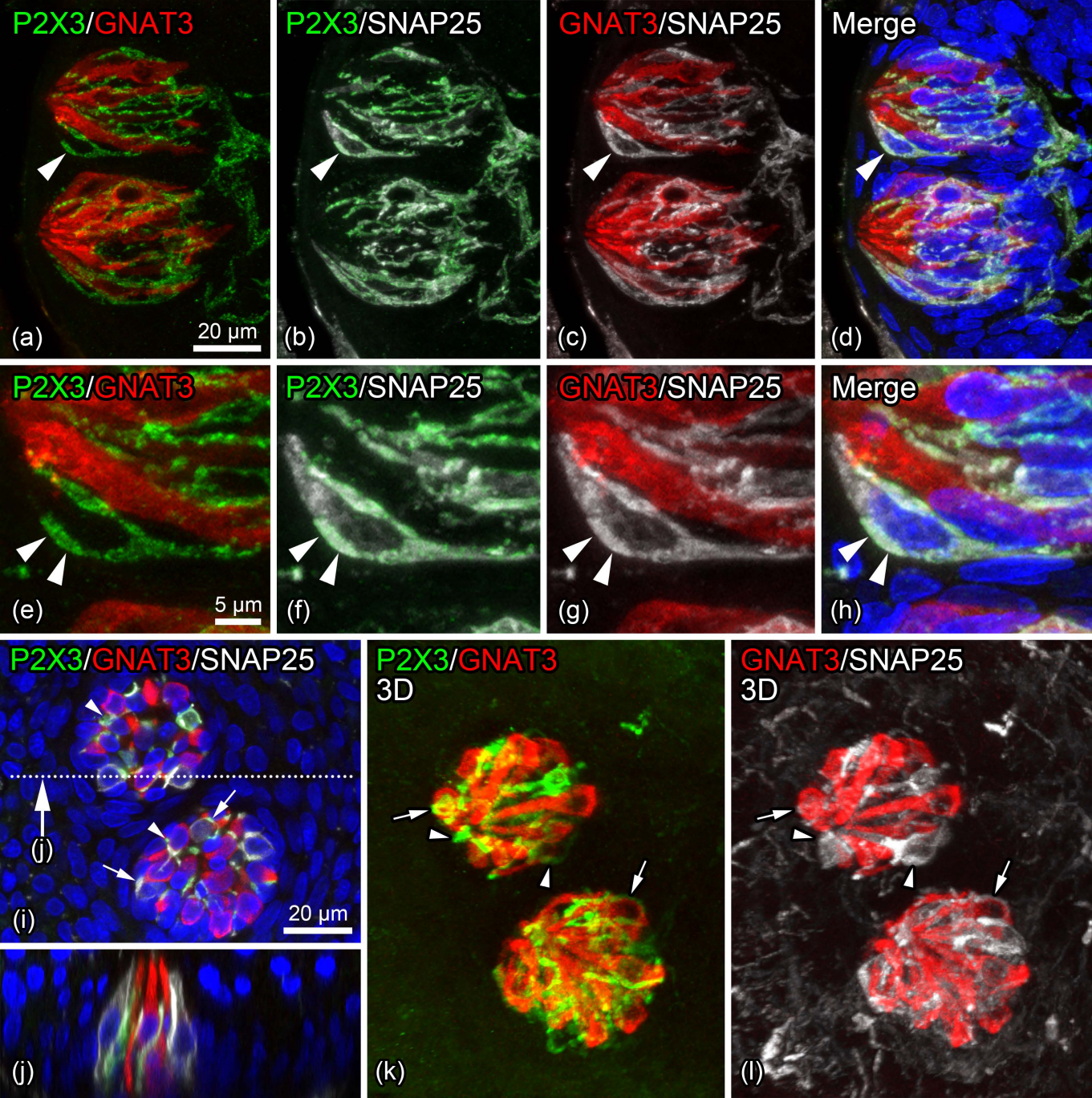
P2X3/GNAT3
P2X3/SNAP25
GNAT3/SNAP25
Merge
(a)
20 µm
(b)
(c)
(d)
P2X3/GNAT3
P2X3/SNAP25
GNAT3/SNAP25
Merge
(e)
5 µm
(f)
(g)
(h)
P2X3/GNAT3/SNAP25
(j)
(i)
20 µm
(j)
P2X3/GNAT3
3D
(k)
GNAT3/SNAP25
3D
(l)

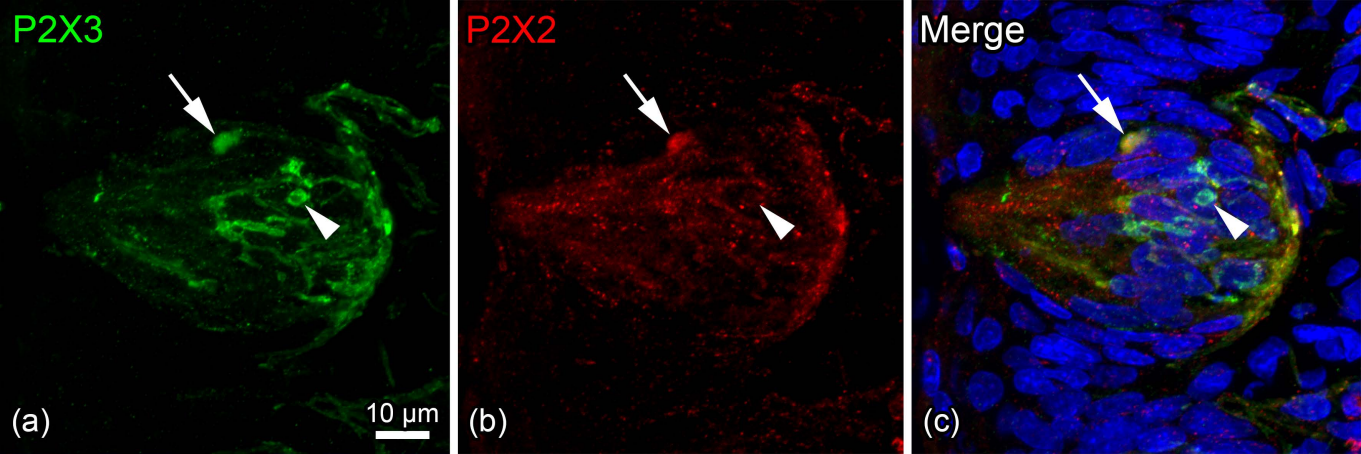
P2X3
P2X2
Merge
(a)
10 μm
(b)
(c)

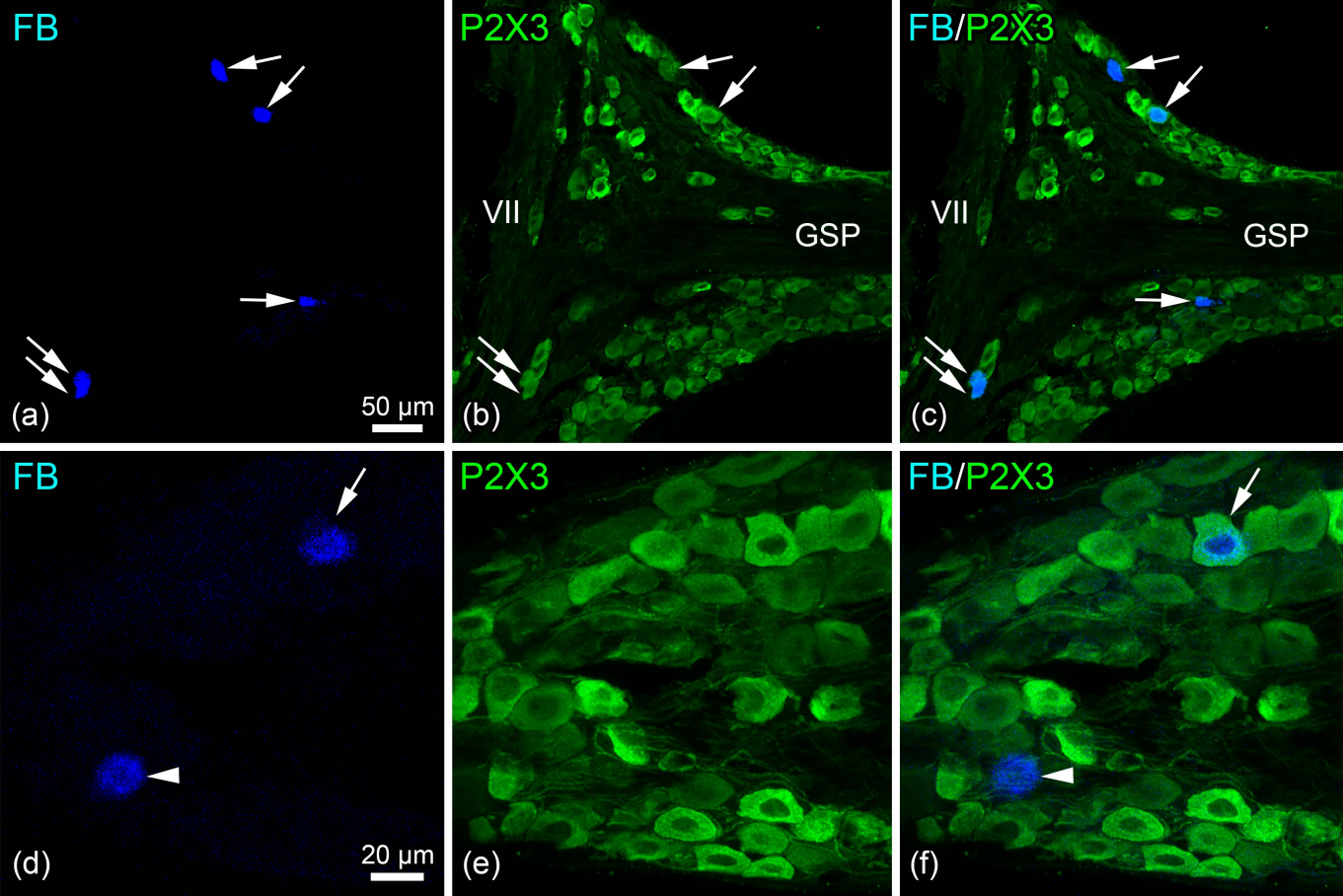
FB
P2X3
FB/P2X3
VII
GSP
VII
GSP
50 μm
(a)
(b)
(c)
FB
P2X3
FB/P2X3
20 μm
(d)
(e)
(f)